applied sciences

MDPI

Article

Fusion Swarm-Intelligence-Based Decision Optimization for Energy-Efficient Train-Stopping Schemes

Xianguang Jia [1], Xinbo Zhou [2], Jing Bao [3,*], Guangyi Zhai [3] and Rong Yan [3]

[1] Faculty of Transportation Engineering, Kunming University of Science and Technology, Kunming 650500, China
[2] Faculty of Information Engineering and Automation, Kunming University of Science and Technology, Kunming 650500, China
[3] Faculty of Civil Aviation and Aeronautics, Kunming University of Science and Technology, Kunming 650500, China
* Correspondence: baojing@stu.kust.edu.cn

Abstract: To solve the decision problem of train stopping schemes, this paper introduces the static game into the optimal configuration of stopping time to realize the rational decision of train operation. First, a train energy consumption model is constructed with the lowest energy consumption of train operation as the optimization objective. In addition, a Mustang optimization algorithm based on cubic chaos mapping, the population hierarchy mechanism, the golden sine strategy, and the Levy flight strategy was designed for solving the problem of it being easy for the traditional population intelligence algorithm to fall into a local optimum when solving complex problems. Lastly, simulation experiments were conducted to compare the designed algorithm with PSO, GA, WOA, GWO, and other cutting-edge optimization algorithms in cross-sectional simulations, and the results show that the algorithm had excellent global optimization finding and convergence capabilities. The simulation results show that the research in this paper can provide effective decisions for the dwell time of trains at multiple stations, and promote the intelligent operation of the train system.

Keywords: golden-sine strategy; Mustang optimization algorithm; population hierarchy mechanism; static game; stopping time optimization

Citation: Jia, X.; Zhou, X.; Bao, J.; Zhai, G.; Yan, R. Fusion Swarm-Intelligence-Based Decision Optimization for Energy-Efficient Train-Stopping Schemes. *Appl. Sci.* **2023**, *13*, 1497. https://doi.org/10.3390/app13031497

Academic Editors: Minvydas Ragulskis, Wen-Hsiang Hsieh and Jia-Shing Sheu

Received: 26 December 2022
Revised: 18 January 2023
Accepted: 20 January 2023
Published: 23 January 2023

1. Introduction

In recent years, urban rail transportation has seen a golden period of development as the scope of urbanization continues to expand, and the travel demand of tourists increases daily. In order to fully meet the travel demand of tourists, urban rail transit has increased the capacity, equipment, scheduling, and operating hours of the system, leading to problems such as operational management difficulties and huge energy consumption in urban rail systems. Regenerative braking technology, as an important part of the process of energy-efficient train operation, provides a practical and less costly solution for energy saving and emission reduction in urban rail transit systems [1]. In a multitrain, multizonal urban rail system, the planning of stopping schemes oriented to regenerative braking directly affects the efficiency of energy saving during train operation, and is the key to decision making in urban rail transportation systems [2].

The main research of the train stopping time planning problem involves the train schedule problem [3]. In order to reflect the real situation of a train stopping, researchers have extended a variety of decision factors. Shi Feng et al. developed an optimal model of stopping time for provincial, local, and county-level stations for different levels of cities where each station is located [4]. Jin GW et al. studied train stopping planning under variable train lengths and stopping times, and constructed a train stopping planning model under stochastic demand [5]. However, all of the above studies only considered objective factors, such as the train itself and the stopping cities, and did not take the core of the problem, i.e., passengers, into account. For this reason, Xu Ruoxi et al. introduced the passenger travel rate into train stopping scheme optimization and constructed a mixed-integer planning model to improve the train's operational efficiency from the passenger's perspective [6]; Qi JG et al. introduced the ideal departure time interval of passengers from the origin station to the destination station into the train stopping scheme, and built an integer linear planning model to fully consider the passengers' demand in real train operation [7]. In summary, in order to explore real and feasible stopping patterns under the influence of objective conditions, this paper focuses on the combination of static-game and train-stopping-time problems.

In the optimization problem of a train stopping scheme, which is essentially an NP-hard problem with high complexity that is difficult to solve, metaheuristic algorithms are mostly used to solve it [8]. Among them, the particle swarm algorithm (PSO) [9] and genetic algorithm (GA) [10] are used to solve the problem. With the increase in problem size and complexity, general metaheuristic algorithms are lacking in convergence accuracy and speed. To further enhance the optimization capability of the algorithm, researchers have introduced hybrid mechanisms based on the metaheuristic algorithm. Qin Jin et al. designed a combined simulated annealing algorithm (CSA), and the experimental simulation results showed its strong solving capability [11]. Zhang Weixiong et al. designed a genetic algorithm based on the ideal-point method on the basis of the genetic algorithm, which effectively solved the problem of the algorithm easily falling into a local optimum. This shows that the use of hybrid metaheuristic algorithms has good benefits for solving large-scale complex optimization problems.

On the basis of the above research, this paper focuses on the train stopping time planning problem involving static games. First, force analysis during train movement was carried out, on which basis an optimization model was established to determine the train stopping time at each stage by introducing the benefit function of the train group–passenger group in the game and discretizing the analysis. Second, the search capability of the algorithm was enhanced by introducing the population hierarchy mechanism, golden sine strategy, and Levy flight strategy on the basis of the classical Mustang optimization algorithm, which reduces the blindness of the algorithm's search while preserving its extensive search capability in order to solve the problem effectively. Further, experiments were conducted with the Shanghai–Nanjing intercity railroad as the simulation background, and compared with existing cutting-edge algorithms; the results show that the designed algorithm had strong robustness and superiority. The research in this paper can provide effective decisions for train stopping times and promote the intelligent development of train systems.

2. Materials and Methods

2.1. Background

The train-stopping-time optimization problem is essentially an NP-hard problem. In the operational strategy, trains can be divided into minimal time and minute operation, and fixed time and minute operation. The latter meets the conditions of energy-saving operation better, and is divided into four main operating states: traction, uniform speed, idling, and braking. The different operating states are subject to different forces: traction, basic resistance, additional resistance (including ramp resistance and curve resistance), and braking force. The continuous problem of train travel is discretized and analyzed by discretely partitioning the train running time. The energy-consumption model of each interval is combined, and waiting time planning based on a static game is introduced to transform single-train single-interval energy consumption into multitrain multi-interval energy consumption; lastly, a multitrain multi-interval energy optimization model with the minimization of energy consumption as the objective function is established.

2.2. Model Assumptions

1. Ignore the shape and size of the trains and treat them as masses to study the state of motion.
2. Each train's right of way is independent and does not interfere with the others.
3. The energy transfer loss between the trains' equipment is constant.
4. The braking regenerative energy can be used immediately.

2.3. Single-Train Single-Interval Energy-Consumption Model

To reduce the complexity of the model, only the traction force, basic resistance, additional resistance (including ramp resistance and curve resistance), and braking force are considered in this paper. According to the Train Traction Calculation Regulations [12], trains of different models have different traction and braking forces, and the standard traction and braking forces are obtained by fitting the data of a certain model train as follows [13]:

$$F_t = \begin{cases} 203\ 0 \le v \le 51.5\ \text{km/h} \\ -0.002032v^3 + 0.4928v^2 - 42.13v + 1314\ 51.5 \le v \le 80\ \text{km/h} \end{cases} \tag{1}$$

$$F_b = \begin{cases} 166\ 0 \le v \le 77\ \text{km/h} \\ 0.1343v^2 - 25.07v + 1300\ 77 < v \le 80\ \text{km/h} \end{cases} \tag{2}$$

where F_t is the traction force (kN), F_b is the braking force (kN), and v is the real-time speed of the train (km/h).

The formula for calculating the resistance of the train during operation is as follows:

$$F_r = F_{bas} + F_{add} \tag{3}$$

$$F_{bas} = \frac{w_0 \times M \times g}{1000} \tag{4}$$

$$w_0 = a + bv + cv^2 \tag{5}$$

$$F_{add} = \frac{M \times g \times (F_{ram} + F_{cur} + F_{tun})}{1000} \tag{6}$$

$$F_{ram} = i = \frac{h}{l} \times 100\% \tag{7}$$

$$F_{cur} = 600/R \tag{8}$$

$$F_{tun} = 0.00013L_{tun} \tag{9}$$

where F_r, F_{bas}, F_{add} are the total resistance, basic resistance, and additional resistance of the train operation, respectively; w_0 is the basic resistance per unit mass of train (N/kN); M is the total mass of train (kg), $g = 9.8\ \text{m/s}^2$. a, b, c are the constants related to the structure determined by the test; F_{ram}, F_{cur}, F_{tun} are the grade resistance, curve resistance, and tunnel resistance of train operation, respectively; i, h, l, R, L_{tun} are the unit grade resistance, elevation difference, distance, curve radius, and tunnel length, respectively.

The differential equation model for single-train operation with the energy-consumption model was obtained by combining the above analyses as follows:

$$\frac{dv}{dt} = \frac{xF_t - yF_b - F_r}{M} \tag{10}$$

$$\frac{ds}{dt} = v \tag{11}$$

$$E_s = \frac{\alpha}{\prod \eta} \frac{dvds}{dtdt} \times Mdt \tag{12}$$

Equation (10) indicates the acceleration of train operation, x, y is a 0–1 variable that varies according to the operating state, traction state $x = 1, y = 0$; inert state $x = 0, y = 0$; braking state $x = 0, y = 1$. Equation (11) indicates the speed of train operation. Equation (12) indicates the energy consumption of a single train in a single zone, α, $\prod \eta$ are the percentage of traction requested by the automatic train operation (ATO) system and the product of energy transfer efficiency of each motor of the train, respectively.

2.4. Static-Game-Based Waiting-Time Planning Model

It is assumed that, in the game of train time formulation, there are two roles, the passenger group and train working group, and the state update of each side in the time formulation game is affected by the situation of the other side, so each side must consider the strategy of the other side to maximize its interests. The time formulation is a precise time point or time interval that is considered to be a static game [14]. The benefits of setting both parties to take time changes are as follows:

$$E_A = A \tag{13}$$

$$\dot{E}_A = \frac{n\binom{k}{n} p^k (1-p)^{n-k} Q_{aver} \triangle t}{Q_e} \tag{14}$$

$$E_B = \mu F_b v \triangle t \tag{15}$$

$$\dot{E}_B = A \tag{16}$$

$$\ddot{E}_A = \frac{n\binom{k}{n} p^k (1-p)^{n-k} Q_{aver} \triangle t}{Q_e} - A \tag{17}$$

$$\ddot{E}_B = \mu F_b v \triangle t - A \tag{18}$$

In Equations (13)–(16), E_A, $\dot{E}_A$, E_B, and $\dot{E}_B$ are the benefits of passenger group selection over the specified delayed $\triangle t$ start, the benefits of passenger group selection over the specified earlier $\triangle t$ start, the benefits of train group selection over the specified delayed A restart, and the benefits of train group selection over the specified earlier $\triangle t$ restart, respectively; in Equations (13) and (16), A is a constant that represents the long-term benefits obtained by a mutual understanding; In Equation (14), $n\binom{k}{n} p^k (1-p)^{n-k}$ denotes the number of passengers satisfying the binomial distribution, Q_{aver} and Q_e are the per ISA income and the price of electric energy, respectively; in Equation (15), μ denotes the conversion efficiency of braking regenerative energy. Equations (17) and (18) represent the benefits obtained in the case of stubbornness when the two parties disagree.

A mixed game is used to solve the Nash equilibrium point, assuming that both sides choose to advance and defer with probabilities P_1 and P_2 with the following equations:

$$\begin{cases} \dot{E}_B P_1 + \ddot{E}_B P_2 = \ddot{E}_A P_1 + E_B P_2 \\ P_1 + P_2 = 1 \end{cases} \tag{19}$$

$$E_{new} = \mu P_2 F_b v \triangle t \tag{20}$$

2.5. Multitrain Multizonal Energy-Consumption Model

On the basis of a single train with a single interval, the energy generated by regenerative braking was taken into account, and the stopping time of stations passed by the train during operation was planned to maximize the use of regenerative braking energy.

$$a_{ti} = a_i \quad i = 0, 1, \ldots, n \tag{21}$$

$$v_{ti} = v_i \quad i = 0, 1, \ldots, n \tag{22}$$

$$s_{ti} = s_i \quad i = 0, 1, \ldots, n \tag{23}$$

Equations (21)–(23) represent the discrete analysis of the continuous problem based on continuous train operation to construct the train operation equations for split time intervals.a_{ti}, v_{ti}, s_{ti} are the initial acceleration, initial velocity, and initial distance of each discrete partition interval, respectively, while a_i, v_i, s_i are the corresponding variables in the interval, and n is the number of partition intervals after discretization.

Combining the models of single-train single-interval and multitrain braking regenerative energy, the multitrain multi-interval energy optimization model was constructed as follows:

$$E_m = \sum_{t=0}^{T} \frac{\alpha}{\prod \eta} \frac{dvds}{dtdt} \times M \triangle t - \sum_{t=1}^{T} \mu P_2 F_b v \triangle t \tag{24}$$

2.6. Wild Horse Optimizer

The established energy consumption optimization model is a nonlinear optimization problem with large-scale combinations for which it is difficult to find the exact feasible solution directly with classical optimization methods in an acceptable amount of time. In contrast, metaheuristic algorithms can solve this problem well with a mechanism based on computational intelligence that can obtain the optimal or approximate solution of the problem with high solution efficiency. According to the literature [15], metaheuristic algorithms are classified into nine categories: biology-based, physics-based, social-based, music-based, chemical-based, sport-based, mathematics-based, swarm-based, and hybrid methods. In this paper, the existing wild horse optimizer (WHO) is improved to solve the developed model. The algorithm is a swarm-based metaheuristic algorithm that finds the optimal solution in space by simulating the population behavior of various types of intelligences, and has good solution performance and efficiency.

The wild horse optimizer is a new population intelligence optimization algorithm proposed by Iraj Naruei et al. in 2021 [16]. It is based on the behavioral characteristics of wild horse populations within and between populations in nature, and has the advantages of easy implementation, fast convergence, and high optimization capability. The algorithm includes various wild horse herd behaviors: herd formation and leader selection, grazing behavior, mating behavior, leader (stallion) leadership team, and leader communication and selection.

2.6.1. Forming the Mustang Herd and Selecting Leaders

Similar to other population intelligence algorithms, the wild horse optimizer randomly generates an initial population within the upper and lower bounds of individuals. The initial population is then divided into G = [N × PS] subpopulations, where PS is the percentage of stallions in the total population, resulting in G stallions that are equally distributed to each wild horse herd.

2.6.2. Grazing Behavior

This phase simulates the grazing behavior of a wild horse herd where each horse considers the stallion as the center of the herd and searches for the optimal solution (grazing) around it, and this process updates each individual (foal or mare) in the way shown in Equation (25).

$$\overline{X}_{i,G}^{j} = 2Z\cos(2\pi RZ) \times (Stallion^j - X_{i,G}^{j}) + Stallion^j \tag{25}$$

$$P = \vec{R}_1 < TDR; IDX = (P == 0); Z = R_2 \otimes IDX + \vec{R}_3 \otimes (\sim IDX) \tag{26}$$

$$TDR = 1 - t \times (\frac{1}{T\_iter}) \tag{27}$$

where $X_{i,G}^{j}$ is the current position of the individual, $X_{i,G}^{j}$ is the updated position of the individual, $Stallion^{j}$ is the stallion position, R is a random number of [–2,2], R_1 and R_3 are the random vectors of [0,1],R_2 is the random number of [0,1], *TDR* is the adaptive parameter, *t* is the current number of iterations, and *T_iter* is the maximal number of iterations.

2.6.3. Horse Mating Behavior

This stage simulates the process of foals mating and producing offspring, where foals leave herd *I* and mate with other foals leaving herd *j* to produce offspring, who then return to herd *k*. The renewal equation for each individual in this process is shown in Equation (28).

$$X_{G,k}^{p} = Mean(X_{G,i}^{q}, X_{G,j}^{z}), i \neq j \neq k, p = q = end \quad (28)$$

where $X_{G,K}^{p}$ denotes the position of foal *p* in group *k* that left the group and re-entered group *k*. The two positions in parentheses denote the positions of its sire and dam, respectively. $X_{G,i}^{q}$ denotes the position of sire *q* that left from group *i*, and $X_{G,j}^{z}$ denotes the position of dam *z* that left from group *j*.

2.6.4. Group Leadership

At this stage, the leader leads the herd to a more suitable habitat where there is competition between different herds. The process is shown in Equation (29).

$$\overline{Stallion_{Gi}} = \begin{cases} 2Z\cos(2\pi RZ) \times (WH - Stallion_{Gi}) + WH, R_3 > 0.5 \\ 2Z\cos(2\pi RZ) \times (WH - Stallion_{Gi}) - WH, R_3 \leq 0.5 \end{cases} \quad (29)$$

where $\overline{Stallion_{Gi}}$ denotes the updated location of the leader, WH is the habitat location, and $Stallion_{Gi}$ is the current location of the leader of the group *i*.

2.6.5. Exchange and Selection of Leaders

At the beginning of the algorithm, leaders (stallions) are generated randomly; during the iteration of the algorithm, leaders are selected iteratively on the basis of the fitness value, as shown in Equation (30).

$$Stallion_{Gi} = \begin{cases} X_{G,i}, fit(X_{G,i}) < fit(Stallion_{Gi}) \\ Stallion_{Gi}, fit(X_{G,i}) > fit(Stallion_{Gi}) \end{cases} \quad (30)$$

2.7. Improved Wild Horse Optimizer

In the traditional wild horse optimizer, each wild horse herd follows its leader in its range to find the optimal solution, which easily leads to the algorithm's total optimal solution; the initial population of the algorithm is generated randomly, which hinders guaranteeing the diversity and uniformity of the population. To address the above problems, this paper introduces cubic chaotic mapping, the population hierarchy mechanism, Levy flight strategy, and golden-sine strategy to effectively improve the solving ability of the algorithm.

2.7.1. Cubic Chaos Mapping

The traditional wild horse optimizer performs optimization by randomly generating the initial population, which leads to individuals being easily concentrated in a few regions, and to the algorithm easily falling into a local optimum later. To address such problems, most studies introduced chaotic mapping mechanisms for improvement [17–20], such as logistic mapping, Fuch mapping, and tent mapping, to enhance the diversity of the initial population and improve the solution efficiency of the algorithm.

In this paper, cubic chaotic mapping is introduced to improve the population initialization strategy of the WHO. The chaotic sequence had better chaotic ergodicity, and the initial wild horse population with more uniform distribution could be obtained by mapping this chaotic sequence into the solution space of wild horse individuals; the standard cubic mapping formula is expressed as follows.

$$X_{n+1} = bX_n^3 - cX_n \tag{31}$$

where X_{n+1} denotes the solution vector of the n-th + 1 individual, and b and c are chaotic constants whose different values affect the range of the mapping.

2.7.2. Population Classification Mechanism

To improve the convergence and global exploitation ability of the wild horse optimization algorithm, a population hierarchy mechanism is introduced to split the wild horse population to find the best solution. All the individuals in the wild horse population are ranked from smallest to largest in terms of fitness: those with higher-than-average fitness are classified as the elite population, while the rest are classified as the inferior population.

A more aggressive perturbation strategy is applied to the inferior population, so that the inferior population can jump out of the current exploration range more quickly, while a milder golden-sine perturbation mechanism is applied to the superior population, which can improve the exploitation of the superior region and prevent the algorithm from falling into a local optimal solution. Through the above population hierarchy mechanism, all individuals are divided into two subpopulations for independent search, which maintains the population diversity without destroying the adaptation degree of dominant individuals.

2.7.3. Levy Flight Strategy

Levy flight, first proposed by French mathematician Paul Levy, is one of the forms of random wandering models. The random wandering step that it provides obeys the Levy distribution, which has a larger tail than those of Gaussian and Cauchy distributions, and thereby has a larger perturbation effect. The Levy flight strategy is well-used in the field of intelligent optimization algorithms [21] and can effectively enhance the global exploration ability of algorithms; it also has a wide range of applications in the fields of physics, biology, statistics, finance, and computer science.

The Levy distribution can be formulated as follows.

$$Levy(\lambda) \sim |s|^{-\lambda} \tag{32}$$

$$s = \mu/|v|^{1/\lambda}, 0 < \lambda < 2 \tag{33}$$

$$\mu \sim N(0, \delta_\mu^2) \tag{34}$$

$$v \sim N(0, \delta_v^2) \tag{35}$$

$$\delta_u = \left\{ \frac{\Gamma(1+\lambda)\sin(\pi\lambda/2)}{2^{(\lambda-1)/2}\Gamma[(1+\lambda)/2]} \right\}^{1/\lambda} \tag{36}$$

$$\delta_v = 1 \tag{37}$$

$$X(t+1) = X(t) + \theta \oplus Levy(\beta) \tag{38}$$

where S is the random walk step, and λ ($1 < \lambda < 3$) is the random exponential parameter. In practical application, the Mantegna method is often used to generate Levy flight random step size s as shown in Equation (33); μ and v are random numbers obeying normal distribution; $\Gamma(x)$ is the gamma function, i.e., $\Gamma(x) = \int_0^\infty t^{x-1}e^{-t}dt$. The population perturbation formula based on Levy the flight strategy is shown in Equation (38); θ is a random number between [0,1], $\oplus$ is a multiplication of elements, β = 1.5.

2.7.4. Gold Sine Strategy

The golden-sine algorithm (Golden SA) is a metaheuristic algorithm based on the sine function model for merit search proposed by Tanyildizi et al. in 2017 [22], which is characterized by few parameters, fast convergence, and high robustness. In this paper, the golden-sine operator in Golden SA is introduced to perturb the individuals in the elite population, and is formulated as follows:

$$X(t+1) = X(t) \times |\sin R_1| + R_2 \times \sin R_1 \times \left| x_1 \times X_{gbest} - x_2 \times X(t) \right| \quad (39)$$

$$\begin{cases} x_1 = -\pi + (1-\tau) \times 2\pi \\ x_2 = -\pi + \tau \times 2\pi \end{cases} \quad (40)$$

$$\tau = (\sqrt{5} - 1)/2 \quad (41)$$

where R_1 is a random number in the range of [0,2π], and R_2 is a random number in the range of [0,π].

2.8. Flowchart of the Improved Wild Horse Optimizer

On the above basis, a flowchart of the wild horse optimizer (IWHO) based on cubic chaos mapping, the population hierarchy mechanism, the golden sine strategy, and the Levy flight strategy is shown in Figure 1.

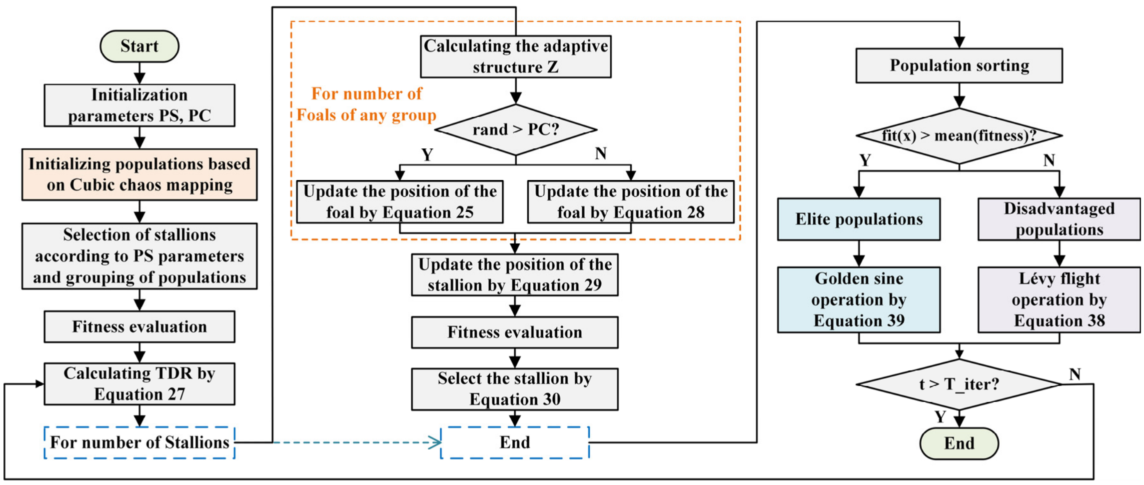

Figure 1. Flowchart of the improved wild horse optimizer.

3. Simulation Analysis

In this paper, we used MATLAB R2022a as the simulation programming tool, Win11 as the operating system, 16 GB of RAM, and NVIDIA GeForce RTX 3050 as the graphics card, and compared the proposed algorithm with the particle swarm algorithm (PSO), genetic algorithm (GA), whale optimization algorithm (WOA), gray wolf optimization algorithm (GWO), and arithmetic optimization algorithm (AOA) for cross-sectional simulation comparison experiments. To ensure the fairness of the experiments, the population size of each algorithm was set to NP = 100.

The maximal number of iterations of each algorithm is used as the termination condition, and the maximal number of iterations T = 200. The population initialization method of each algorithm, i.e., the way to obtain the starting search point of the algorithm, is based on the standard form in which the algorithm is first proposed.

The parameters of each algorithm were set as follows: in PSO, learning factor $c1 = c2 =$ 1.5, maximal particle velocity $Vmax$ = 10, minimal velocity $Vmin = -10$; in GA, crossover probability Pc = 0.8, variation probability Pm = 0.1; in GWO, convergence factor a = 2; in AOA, maximal value MOP_Max = 1, minimal value MOP_Min = 0.2, control parameter μ = 0.499, and sensitivity parameter α = 5 for the acceleration function. On the basis of web data, assumptions were made for some of the parameters in the model: braking regenerative energy conversion efficiency μ = 70%, A = 1000, Q_{aver}= 5000 RMB/month, Q_e= 0.52 RMB/kWh, and maximal waiting time T_w = 40 min. The Shanghai–Nanjing intercity railroad line data as shown in Table 1 were imported into the model for simulation. Each algorithm was independently run 20 times, and the simulation results are shown in Figures 1–3, Tables 2 and 3.

Table 1. Shanghai–Nanjing intercity railroad line data.

Serial Number	Station Name	Mileage (km)	Serial Number	Station Name	Mileage (km)	Serial Number	Station Name	Mileage (km)
1	Shanghai Station	0	8	Suzhou Park Station	74.3	15	Changzhou Station	165.5
2	Shanghai West Station	5.3	9	Suzhou Station	83.9	16	Danyang Station	209.6
3	Nanxiang North Station	14.4	10	Suzhou New District Station	94.4	17	Dandong Station	224.5
4	Anting North Station	29.2	11	Wuxi New District Station	113.2	18	Zhenjiang Station	237.5
5	Huaqiao Station	40.5	12	Wuxi Station	126.1	19	Baohuashan Station	274
6	Kunshan South Station	50	13	Huishan Station	139.8	20	Xianlin Station	288
7	Yangcheng Lake Station	59.2	14	Qishuyan Station	154.1	21	Nanjing Station	300.2

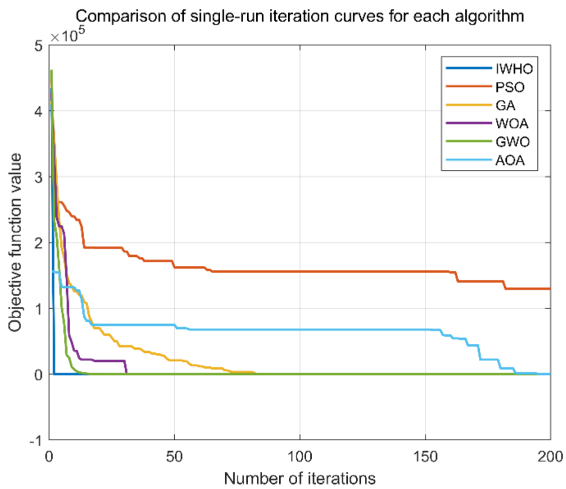

Figure 2. Objective function convergence curves for each of the six algorithms in a single run.

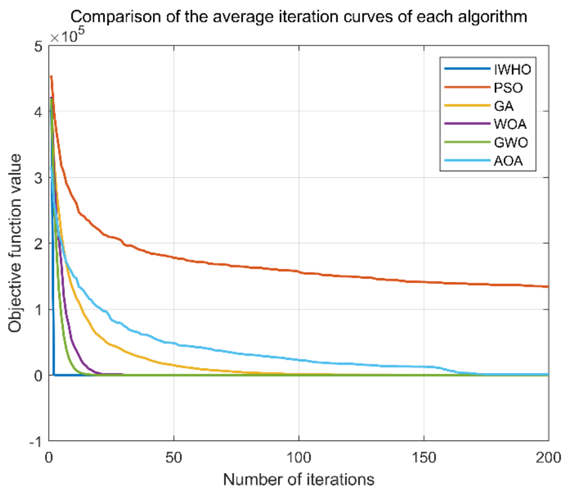

Figure 3. Average objective function convergence curves for each of the six algorithms over 20 runs.

Table 2. Comparison of the average fitness values of each algorithm.

Algorithm	IWHO	PSO	GA	WOA	GWO	AOA
Average fitness value	$-1.3574 \times 10^{-11.}$	1.3490×10^5	5.4600×10	-1.3574×10^{-11}	-9.6057×10^{-12}	2.9309×10^3

Table 3. Optimal waiting strategy for each algorithm in one randomized run.

Algorithm \ Site Number	1	2	3	4	...	17	18	19	20
IWHO/ (minute)	40	0	0	0	...	0	0	0	0
PSO /(minute)	14.4681	13.0378	2.4756	10.2296	...	1.2553	12.1705	0.0566	2.8871
GA /(minute)	40	0	0	0	...	0	0	0	0
WOA /(minute)	40	0	0	0	...	0	0	0	0
GWO /(minute)	1.1384	3.4957×10^{-16}	1.8316×10^{-16}	9.3486×10^{-17}	...	1.0886×10^{-16}	1.2695×10^{-16}	0	1.1867×10^{-16}
AOA /(minute)	0	40	0.0529	0.0065	...	0	0	0	0.0269

From the iteration curves of each algorithm in Figures 1 and 2, it can be intuitively seen that the improved wild horse optimizer (IWHO) proposed in this paper was clearly comparable to similar algorithms in terms of convergence capability and solution efficiency for both a single run and multiple runs to take the average results. As seen from the numerical simulation results in Tables 2 and 3, IWHO also performed well compared to similar algorithms in terms of solution accuracy and quality, with the average objective function value of -1.3574×10^{-11} being the optimal value among the comparison algorithms, and the values of the feasible solutions were all integers. In summary, from the perspectives of both qualitative and quantitative analysis, the IWHO proposed in this paper had greater advantages for solving the described model. The optimal objective function value obtained from the simulation experiment was -1.3575×10^{-11}; the optimal waiting strategy was no waiting was performed for all station gaps except for 40 min at the first station gap.

4. Discussion

By comparing it with the other five algorithms, the IWHO algorithm had a strong advantage in search capability and running time, especially since the convergence adaptation in 20 runs was significantly higher than that of the other algorithms, and it was not easy for it to fall into the local optimal solution. The real data of the line for the simulation of the stopping scheme show that the IWHO algorithm had a better effect on energy saving compared with that of the other five algorithms. Therefore, the IWHO algorithm could contribute to the train-stopping decision problem in urban rail transportation systems, greatly reducing resource consumption and improving overall efficiency.

5. Conclusions

In this paper, the decision problem of train stopping scheme was studied. On the basis of the static game, a train-stopping-time allocation model was constructed with the lowest operating energy consumption as the optimization objective. On the basis of the standard Mustang optimization algorithm, cubic chaos mapping, the population hierarchy mechanism, the golden sine strategy, and the Levy flight strategy were introduced to improve the global optimization capability of the algorithm. In addition, simulation experiments were conducted on the basis of actual data of the Shanghai–Nanjing intercity railroad, and the comparison with existing cutting-edge algorithms showed that the introduced improvement strategies could render the algorithm more robust and superior in solving complex high-latitude problems. The model constructed in this paper is effectively applicable to the decision problem of train stopping duration at multiple stations, and can be extended to the field of long-distance multisite train stopping decisions such as urban rail and light rail. However, due to the constraints of this paper, the passengers were idealized, and further social research will be conducted to improve the rationality of the game in future studies.

Author Contributions: Conceptualization, X.J.; methodology, J.B. and X.Z.; software, X.Z. and J.B.; validation, G.Z., J.B. and R.Y.; formal analysis, X.J. and G.Z.; resources, J.B. and X.J.; data curation, X.J.; writing—original draft preparation, R.Y.; writing—review and editing, J.B.; visualization, J.B. and R.Y. All authors have read and agreed to the published version of the manuscript.

Funding: This work was supported in part by the Science and Technology Project of China Southern Power Grid Co., Ltd. under grant YNKJXM20220174.

Institutional Review Board Statement: Not applicable.

Informed Consent Statement: Not applicable.

Data Availability Statement: Data are contained within the article.

Conflicts of Interest: The authors have no conflict of interest regarding this paper.

References

1. Scheepmaker Gerben, M.; Goverde Rob, M.P. Energy-efficient train control using nonlinear bounded regenerative braking. *Transp. Res. Part C: Emerg. Technol.* **2020**, *121*, 102852. [CrossRef]
2. Pan, D.; Zhao, L.; Luo, Q.; Zhang, C.; Chen, Z. Study on the performance improvement of urban rail transit system. *Energy* **2018**, *161*, 1154–1171. [CrossRef]
3. Niu, H. Literature Review on Rail Train Timetabling Problems. *J. Transporation Syst. Eng. Inf. Technol.* **2021**, *21*, 114–124.
4. Feng, S.; Zhenyi, L.; Shuo, Z.; Xinghua, S. Optimization Method for Train Passing-Stopping Ratio under Passenger Travel Demand Agglomeration of High Speed Railway. *China Railw. Sci.* **2017**, *38*, 121–129.
5. Jin, G.; He, S.; Li, J.; Guo, X.; Li, Y. An Approach for Train Stop Planning With Variable Train Length and Stop Time of High-Speed Rail Under Stochastic Demand. *IEEE Access* **2019**, *7*, 129690–129708. [CrossRef]
6. Ruoxi, X.; Lei, N.; Huiling, F. Train Stop Plan Optimization of High-speed Rail for Improving Passenger Travel Efficiency. *J. Transporation Syst. Eng. Inf. Technol.* **2020**, *20*, 174–180.
7. Jianguo, Q.; Valentina, C.; Lixing, Y.; Chuntian, Z.; Zhen, D. An Integer Linear Programming model for integrated train stop planning and timetabling with time-dependent passenger demand. *Comput. Oper. Res.* **2021**, *136*, 105484.
8. Dong, X.; Li, D.; Yin, Y.; Ding, S.; Cao, Z. Integrated optimization of train stop planning and timetabling for commuter railways with an extended adaptive large neighborhood search metaheuristic approach. *Transp. Res. Part C: Emerg. Technol.* **2020**, *117*, 102681. [CrossRef]
9. Zhang, Y.; Zuo, T.; Zhu, M. Research on multi-train energy saving optimization based on cooperative multi-objective particle swarm optimization algorithm. *Int. J. Energy Res.* **2021**, *45*, 2644–2667. [CrossRef]
10. Lianhua, T.; Andrea, D.; Xingfang, X.; Yantong, L.; Xiaobing, D.; Marcella, S. Scheduling local and express trains in suburban rail transit lines: Mixed-integer nonlinear programming and adaptive genetic algorithm. *Comput. Oper. Res.* **2021**, *135*, 105436.
11. Jin, Q.; Xiqiong, L.; Kang, Y.; Guangming, X. Joint Optimization of Ticket Pricing Strategy and Train Stop Plan for High-Speed Railway: A Case Study. *Mathematics* **2022**, *10*, 1679.
12. Hu, P.; Chen, R.; Li, H.; Liang, Y. Train Operation Traction Energy Calculation and Saving in Urban Rail Transit System. Second international conference on instrumentation, measurement, computer, communication and control. *Inst. Electr. Electron. Eng.* **2012**, 505–507. [CrossRef]
13. Hongguo, S.; Oiyuan, P.; Hanying, G. Traction calculation model of urban mass transit. *J. Triffic Transp. Eng.* **2005**, *5*, 20–26.
14. Mohtadi, M.M.; Nogondarian, K. Presenting an algorithm to find Nash equilibrium in two-person static games with many strategies. *Appl. Math.* **2015**, *251*, 442–452. [CrossRef]
15. Akyol, S.; Alatas, B. Plant intelligence based metaheuristic optimization algorithms. *Artif. Intell. Rev.* **2017**, *47*, 417–462. [CrossRef]
16. Naruei, I.; Keynia, F. Wild horse optimizer: A new meta-heuristic algorithm for solving engineering optimization problems. *Eng. Comput.* **2022**, *38*, 3025–3056. [CrossRef]
17. Varol Altay, E.; Alatas, B. Bird swarm algorithms with chaotic mapping. *Artif. Intell. Rev.* **2020**, *53*, 1373–1414. [CrossRef]
18. Arora, S.; Anand, P. Chaotic grasshopper optimization algorithm for global optimization. *Neural Comput. Appl.* **2019**, *31*, 4385–4405. [CrossRef]
19. Wang, J.; Li, Y.; Hu, G.; Yang, M. An enhanced artificial hummingbird algorithm and its application in truss topology engineering optimization. *Adv. Eng. Inform.* **2022**, *54*, 101761. [CrossRef]
20. Deng, H.; Liu, L.; Fang, J.; Qu, B.; Huang, Q. A novel improved whale optimization algorithm for optimization problems with multi-strategy and hybrid algorithm. *Math. Comput. Simul.* **2023**, *205*, 794–817. [CrossRef]

21. Zheng, J.; Zhan, H.; Huang, W.; Zhang, H.; Wu, Z. Development of Lévy Flight and Its Application in Intelligent Optimization Algorithm. *Comput. Sci.* **2021**, *48*, 190–206.
22. Tanyildizi, E.; Demir, G. Golden sine algorithm: A novel math-inspired algorithm. *Adv. Electr. Comput. Eng.* **2017**, *17*, 71–78. [CrossRef]